



Designed a Resonance Rayleigh Scattering (RRS) Spectroscopic Technique for the Selective Determination of Acetaminophen Drug in Human Fluid Samples by Using Chitosan-capped Gold Nanoparticles

Kobra Moteabbed, Jafar Burromandpiroze *, Vahid Zare- Shahabadi, Soheil Sayyahi

Department of Chemistry, Mahshahr Branch, Islamic Azad University, Mahshahr, Iran

(Received 05 Feb. 2023; Final revised received 18 May 2023)

Abstract

The interaction of acetaminophen drug by chitosan-capped gold Nanoparticles was investigated using a resonance Rayleigh scattering (RRS) spectroscopic technique. The standard deviation of (1.1 %), and detection limit of the method (0.5 ng mL^{-1} in time 6 min, 325 nm) were obtained for sensor level response chitosan-capped AuNPs with (97%) confidence evaluated. The results indicated that this method had good selectivity in the presence of coexisting compounds. The scattering intensity (ΔI_{RRS}) was linearly dependent on acetaminophen drug concentration over the range (0.5 to 200.0 ng mL^{-1}) with a determination coefficient (r) of 0.998. This method could be suitably used for analysis of acetaminophen drug in pharmaceutical, human fluid, and other drugs, and hospital samples.

Keywords: Acetaminophen (AP) Drug, Chitosan-capped AuNPs, Determination, Human Fluid samples, Resonance Rayleigh Scattering (RRS) method.

**Corresponding author: Jafar Burromandpiroze, Department of Chemistry, Mahshahr Branch, Islamic Azad University, Mahshahr, Iran. Email: jafarburromandpiroze72@gmail.com.*

Introduction

Acetaminophen (AP) is a common analgesic, and antipyretic drug which is prescribed, and purchased over the counter for the relief of minor pain such as fever and headaches. AP has no toxic effect in normal therapeutic doses while large doses particularly with simultaneous consumption of alcohol or other drugs can cause nephrotoxicity, skin rashes, and inflammation of the pancreas, and liver disorders [1-3]. In that respect, for tracing one medicament in pharmaceutical, and biological samples, for discerning, and accurate reorganization of species (1-inorganic 2-organic and 3- biomolecules) in different intricate matrices, and determining environmental pollution caused by drugs in pharmaceutical and biological samples attention has been using of spectrometric method, and by sensors metal nanoparticles sensor [4-7].

Due to the profitable application of metal nanoparticles, technologies have taken advantage of nanoscale materials in a variety of fields from chemistry to medicine [8,9]. Recovery of nanoparticles from plant tissue is tedious, expensive, and requires enzymes to destroy plant cellulose tissue. Therefore, used the Small molecular polymer substrates in low processing, and large scale to prepare various metal nanoparticles [10-13]. The forms, sizes, and structures of metallic materials which are extensively linked to their chemical, physical, and optical characteristics, set the ground for successful use of them in technologies. Among metals nanostructures features, their optical properties have been the main focus of methods such as Localized Surface Plasmon Resonance (LSPR). LSPR relies on the overall oscillation of electrons that may appear in the spectrum may be featured as visible to near-UV region [14,15]. It is in this respect that study of these particles, and their characterization has become a pivotal research area in materials [16]. Chitosan-capped AuNPs have very interesting features among of the Surface Plasmon resonance (SPR), and/or Resonance Rayleigh Scattering (RRS) can be highlighted. These two methods have different applications in many fields of research [17,18]. The followings have made (chitosan-capped AuNPs) a new class of probes: 1. Their unique surface plasmon 2.Their optical properties [19,20]. Herein, chitosan-capped AuNPs with were synthesized successfully for the fabrication of sensitive, and specific sensor toward (AP) drug. As shown in (Figure 1), AuNPs nanoparticles led to the formation of chitosan-capped AuNPs - (AP) drug assembly in the presence. This study aimed to find a simple, fast, and very sensitive method for identifying, and measuring the (AP) drug by chitosan-capped AuNPs sensor. Various effective factors such as (pH, (AP) drug concentration, chitosan-capped AuNPs concentration, time reaction, etc.) on the response of the method and obtaining the optimal test values, and accuracy of the method presented in the measurement of (AP) drug as well as comparing the performance of the method with routine clinical techniques and checking the accuracy of the method, the identification, and measurement of

(AP) drug by a Resonance Rayleigh Scattering new method in urine, and blood serum samples. The chemical chitosan-capped AuNPs sensor made it possible as an excellent sensor with reproducibility, good recovery and a very low detection limit for measuring (AP) drug. The method by Resonance Rayleigh Scattering introduced to measure (AP) drug in real samples such as urine, and blood can be used for hospital samples.

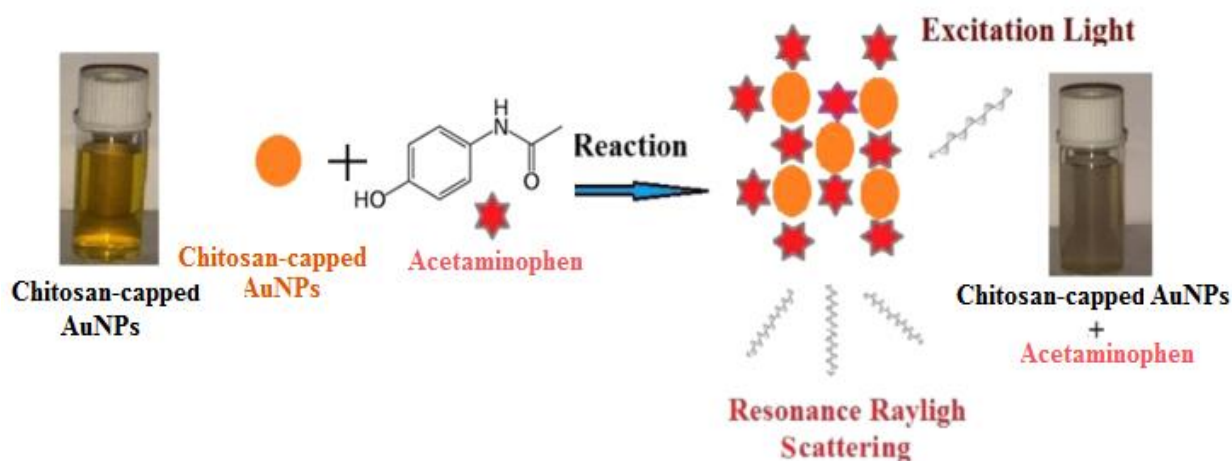


Figure 1. Schematic of reaction of the chitosan-capped AuNPs with (AP) drug insecticide which produces chitosan-capped AuNPs - (AP) drug cluster at pH 6.

Experimental

Materials and Instrumentation

All chemicals including (HAuCl₄) (98%), Chitosan (99%), were provided from Merck Company while acetaminophen (AP) drug (98.0%) was purchased from (Razi Company, Iran). Buffer solutions with pH < 7.0 were prepared using 1 mL of boric acid–acetic acid–phosphoric acid (1.0 M), and pH > 7.0 was adjusted by the addition of 0.2 M sodium hydroxide. UV–visible spectra, Maya Pro 180 spectrophotometer (Shimadzu Company, Japan). Fourier transform infrared spectra (FT-IR) were obtained on a (PerkinElmer FT-IR spectrum BX, Germany). X-ray diffractometer with Cu K α radiation at beam acceleration conditions of 40 kV/35 mA. The pH was measured using an Inolab wtw720 (Germany).

Resonance Rayleigh scattering (RRS)

Resonance Rayleigh Scattering (RRS) is a process produced by the resonance of scattering and absorption of light when the wavelength of RRS is located at or close to its molecular absorption band. RRS, when a particle is exposed to an electromagnetic radiation, the electrons in the particle oscillate at the same frequency as the incident wave. Resonance Rayleigh scattering takes place

when the wavelength of Rayleigh scattering is located at or close to the molecular absorption band. The properties of scattered light depend on the size, composition, shape, homogeneity of the nanoparticles, and refractive index of the medium [16,17].

Pretreatment of real samples

In a 100 mL beaker, treatment of a 50 mL portion of a human fluids (urine or blood) samples (or a spiked human fluids samples) in hospitals Ahvaz were done using 2 mL of concentrated HNO₃ (63%) and an HClO₄ (70%) mixture of 2:1 and then covered with a watch glass. for 10 min, and then with the help of a 100 mL volumetric flask, desired. 5 mL of the obtained clear solution was picked, and the analysis acetaminophen drug by standard addition method procedure [21].

Synthesis of chitosan-capped AuNPs

In this regard, the following details of the materials are important to consider in their synthesis: surface property, size distribution, apparent morphology, particle composition, dissolution chitosan-capped AuNPs by the reduction of HAuCl₄ as a modifier according to the method in the literature [22]. Briefly, 10.0 mL chitosan (2.0 mM) solution into the reaction flask that contained 1.0 mL of HAuCl₄ (2.0 mM) under vigorous stirring. After 15 min into the above solution at room temperature, and stirred for 1 h. UV–Visible spectrum of chitosan-capped AuNPs. The inset picture shows chitosan-capped AuNPs. The dark colloidal solution color was changed to bright yellow, confirming that the formation of chitosan-capped AuNPs. The chitosan-capped AuNPs solution was stored in the dark at $4.0 \pm 2.0^\circ\text{C}$ to remain stable for several weeks (Figure 2).

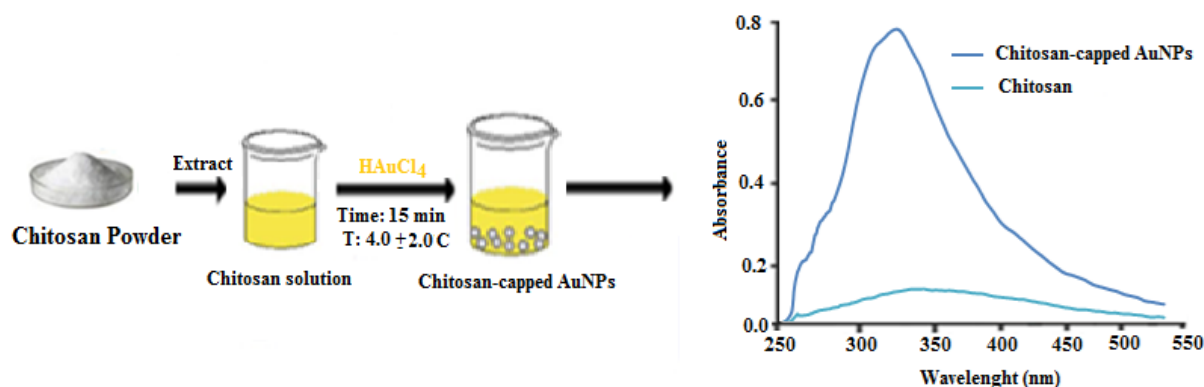


Figure 2. Synthesis of chitosan-capped AuNPs.

General procedure

In this procedure, 1 mL prepared chitosan-capped AuNPs solution (50 ng mL^{-1}), 1 mL of phosphate buffer (pH 6.0) and different concentrations of (AP) drug to 10 mL volumetric flasks, and diluted with double distilled water. The difference between the quantities of the absorption in a wavelength equal to (325 nm) in a time interval equal to (5.0 min). By adding (AP) drug to the solution, it was observed that resonance Rayleigh scattering (RRS) of the solution of chitosan-capped AuNPs at wavelength of (325 nm) dropped. All reaction steps were repeated by increasing (AP) drug concentration by 20.0 ng mL^{-1} every 10 s. During the scattering intensity (ΔI_{RRS}) detection of (AP) drug (ΔI), a blank sample (I_0) was also analyzed [23,24]. There was a sharp change in the resonance Rayleigh scattering of the sensor in the 325 nm region, a continuous increase in (AP) drug intensity at intervals of 10 s in solution, and changes in the resonance Rayleigh scattering of the sensor. Peak scattering intensity at 375 nm with an increase in resonance Rayleigh scattering (ΔI_{RRS}) can be seen in the UV-visible spectrum given in (Figure 3).

Finally, the resonance Rayleigh scattering obtained for (AP) drug sample was subtracted from intensity of the blank sample. The spectrum changes occurred due to the addition of (AP) drug in the range of (20 ng mL^{-1} at 200 ng mL^{-1}), and the formation of a complex. As can be seen, the complex ((AP) drug–sensor) has two absorption peaks at the wavelengths of 325 and 420 nm (Figure 4) [23,24].

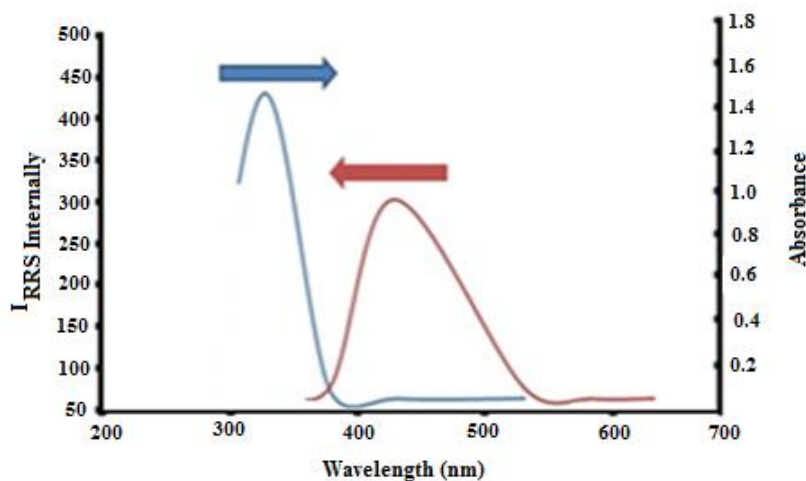


Figure 3. Scattering intensity (ΔI_{RRS}) spectra detection of (AP) drug by chitosan-capped AuNPs (line blue) and UV-visible spectrum (line red). The apparent spectral evolution including the formation of a well-defined isobestic point at around (375 nm) was estimated.

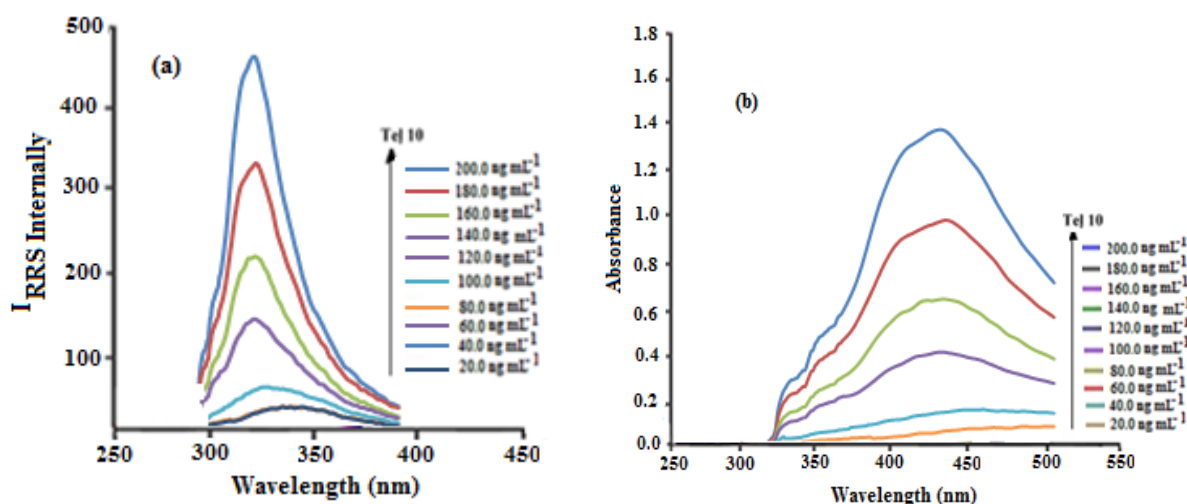


Figure 4. (a) Scattering intensity (ΔI_{RRS}) spectra detection of (AP) drug by chitosan-capped AuNPs in 325 nm; and added solution increasing of the (AP) drug (20.0 ng mL^{-1}) in time 30 s. (b) The absorption spectra of (AP) drug by chitosan-capped AuNPs added solution increasing of the (AP) drug solution (20.0 ng mL^{-1}) in time 30 s. [50.0 ng mL^{-1} of chitosan-capped AuNPs, pH 6.0, time 5.0 min and phosphate buffer solution].

Results and discussion

Characterization

In Figure 5a, the FTIR spectrum of activated carbon prepared from chitosan-capped AuNPs is shown. Additionally, the observed absorption signal at 3451 cm^{-1} points to O-H groups' presence because of the alcoholic or phenolic functional groups. Also, the presence of C-H groups is well proven by the signal observed at 2930 cm^{-1} . Correspondingly, the C=C active group's presence is confirmed by the signal observed 1568 cm^{-1} , the signal at 776.8 cm^{-1} is relevant to the Au-O group of the chitosan-capped AuNPs [25]. Different X-ray emission peaks are chitosan-capped AuNPs shown in (Figure 5b). The signals at 38.5 (122), 45.0 (111), 52.2 (200), 54.4 (231), and 72.7 (220) are ascribable to diffractions and reflections from the carbon atoms [26]. The perfect crystalline nature of the material was proven after functionalizing with chitosan-capped AuNPs. However, the great intensity of the signal at 45.0 (111) confirmed that there has been a slight amount of material in an amorphous state. The morphological properties of the samples scrutinized by SEM are exhibited. By looking at (Fig. 5c). After surface modification, the chitosan-capped AuNPs became uneven, larger, and bundled [26,27]. EDX (energy-dispersive X-ray spectroscopy) spectrum of the EDX spectrum recorded from a film, after formation of chitosan-capped AuNPs shown in (Fig. 5d) [27].

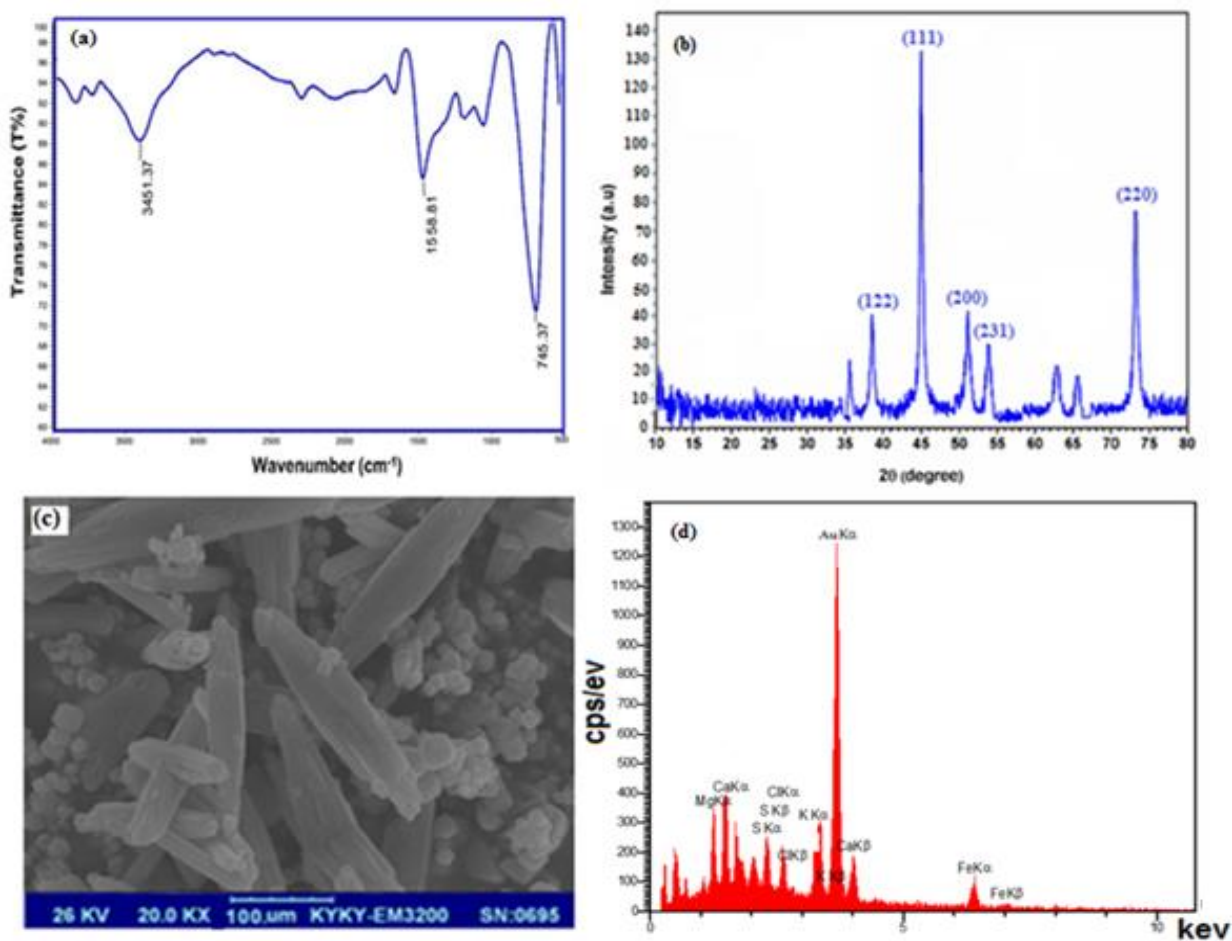


Figure 5. (a) FT-IR transmittance spectrum (b) Different X-ray emission peaks (c) The (SEM) image of the prepared (d) EDX transmittance spectrum are Chitosan-capped AuNPs.

Scattering intensity (ΔI_{RRS}) spectra for determination of (AP) drug by chitosan-capped AuNPs and presence 50 ng mL^{-1} of (AP) drug

The scattering intensity (ΔI_{RRS}) spectra of the solution after adding each analyte, distinct stripping peaks can be seen for (AP) drug in the peak separation of at wavelength range of 300–350 nm. This peak was attributed to facilitating electron transfer between (AP) drug, and chitosan-capped AuNPs [28]. The scattering intensity (ΔI_{RRS}) spectra is dependent on many factors including pH of solution, time, and the instrumental parameters of scattering intensity (ΔI_{RRS}) spectra in the lowest detection limit, based on these observations, the scattering intensity of the chitosan-capped AuNPs is greatly increases after the addition of (AP) drug, and the maximum difference between scattering signals from chitosan-capped AuNPs at wavelength range of 300–350 nm, and the scattering intensity (ΔI_{RRS}) complex (chitosan-capped AuNPs –(AP) drug) is located at 325 nm is shown in (Figure 6). The chitosan-capped AuNPs can be useful for determination of (AP) drug in samples [29].

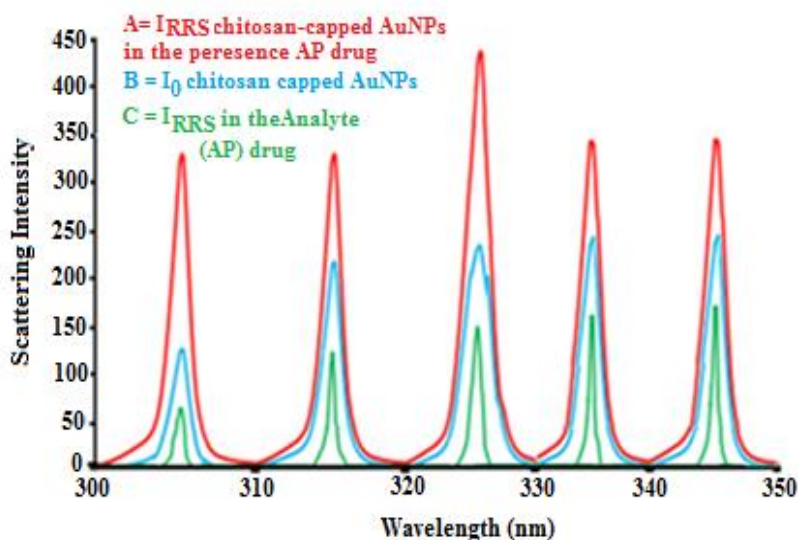


Figure 6. Overlaid scattering intensity spectra of the chitosan-capped AuNPs, chitosan-capped AuNPs-(AP) drug complex, and (AP) drug at wavelength range of 300–360 nm.

Optimization of sensing conditions parameters on the resonance Rayleigh scattering

Obtaining an exceptionally sensitive response in detecting (AP) drug rests upon the systematic optimization of pH values, chitosan-capped AuNPs and incubation time.

Impact of buffer

In this section, the best type of buffer (citrate, acetate, and phosphate buffer), and its volume for maximum of (AP) drug availability for detection purpose with chitosan-capped AuNPs are investigated. Furthermore, 1.0 mL of 0.1 M phosphate buffer the optimal buffer, and as a supporting electrolyte medium in different concentrations of (AP) drug was selected as optimum [30].

Impact of pH

According to data, pH 6.0 produced the best results as compared to other pH values among the pH range from 2 to 8. Thus, this pH could be useful for stability of deposited chitosan-capped AuNPs, and provision of maximum of (AP) drug availability for detection purpose, shown in (Figure 7) [30,31].

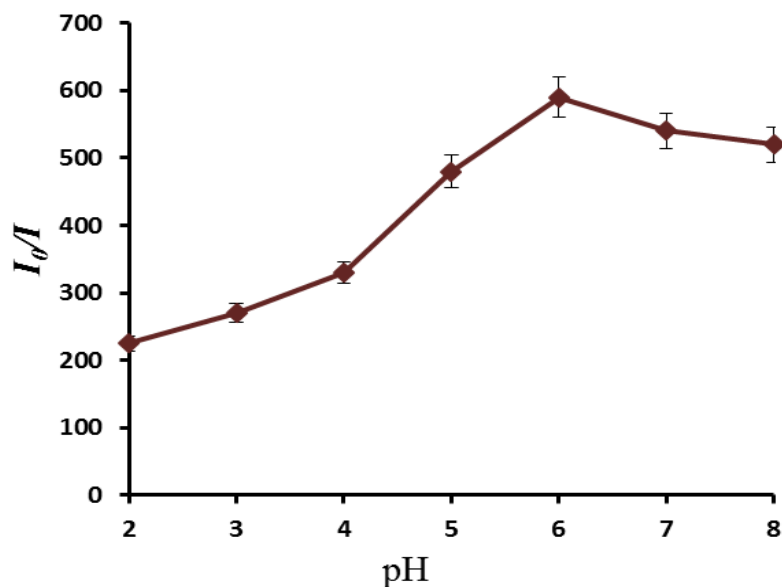


Figure 7. Effect of pH on the scattering intensity (ΔI_{RRS}) [aqueous sample volume, 10 mL, chitosan-capped AuNPs concentration, 50 $\mu\text{mol L}^{-1}$, (AP) drug = 100.0 ng mL^{-1}].

Impact of chitosan-capped AuNPs

The effect of chitosan-capped AuNPs concentration on the stability of scattering intensity was studied. The results showed that the scattering intensity (ΔI_{RRS}) reached a maximum at 50 ng mL^{-1} concentration chitosan-capped AuNPs after all reagents were added, and a standing 50 ng mL^{-1} concentration chitosan-capped AuNPs was selected for further works, shown in (Figure 8) [32].

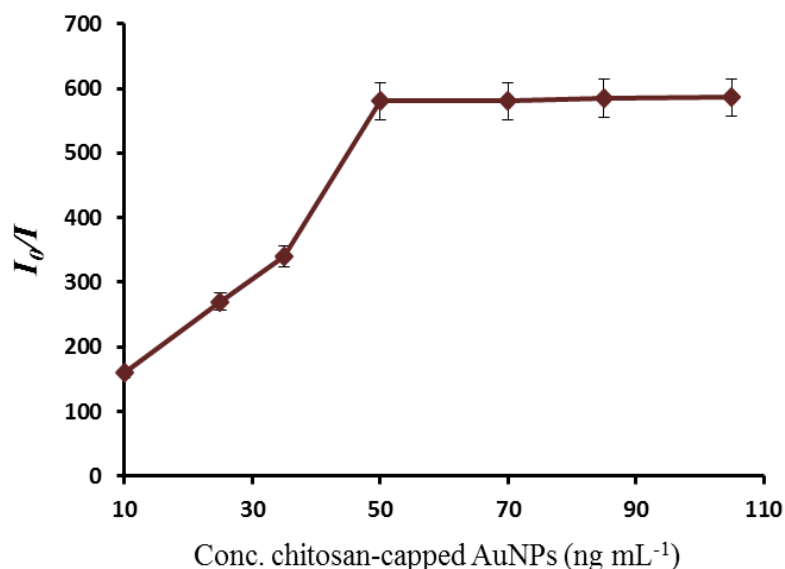


Figure 8. Effect of chitosan-capped AuNPs on the scattering intensity (ΔI_{RRS}) [aqueous sample volume, 10 mL, pH=6, time = 5 min, (AP) drug = 100.0 ng mL^{-1}].

Impact of addition and standing time

The effect of standing time on the stability of scattering intensity was studied. The results showed that the scattering intensity (ΔI_{RRS}) reached a maximum at 5 min after all reagents were added, and it remained stable for over 8 min without any change significant, shown in (Figure 9) [17,33].

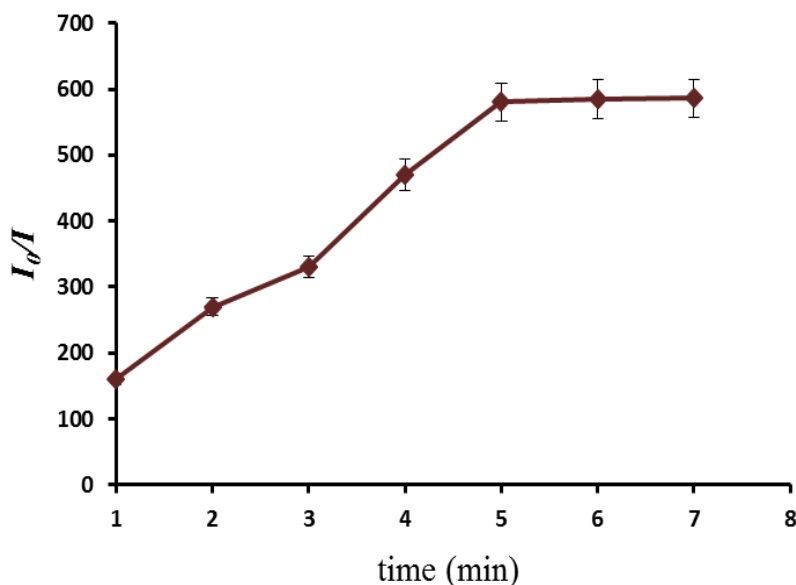


Figure 9. Effect of time on the scattering intensity (ΔI_{RRS}) [aqueous sample volume, 10 mL, chitosan-capped AuNPs concentration, 50 $\mu\text{mol L}^{-1}$, pH=6, (AP) drug = 100.0 ng mL^{-1}].

Calibration curve

The excellent catalyst activity of the chitosan-capped AuNPs, which was examined in the previous sections, makes it possible to measure (AP) drug at low concentrations. For this purpose, and for the analysis of solutions, first it is necessary to prepare a calibration curve to use it to measure the concentration of unknown samples [14,33]. To prepare the calibration curve, solutions with different concentrations of (AP) drug (from 0.5 to 200.0 ng mL^{-1}), and their resonance Rayleigh scattering technique, which is shown in (Figure 10a). It can be seen that as the concentration of (AP) drug gradually increases, its peak resonance of scattering, and absorption of light current also increases, and there is a direct, and linear relationship between the concentration, and the peak scattering intensity (ΔI_{RRS}), and absorption of light current, which is the (AP) drug calibration equation shown in (Figure 10b). The Limit of Detection (LOD) of the modified chitosan-capped AuNPs and (AP) drug was calculated based on three times of standard deviation of the blank signals to calibration slope ($3S/m$). LODs were calculated (0.5 ng mL^{-1}) for (AP) drug. The precision of the method was evaluated by performing ($n=7$) replicate measurements of solutions containing 100.0 ng mL^{-1} of (AP) drug, and the relative standard deviations (RSD) for these determinations were (1.1 %), respectively (Figure 10b) [34,35].

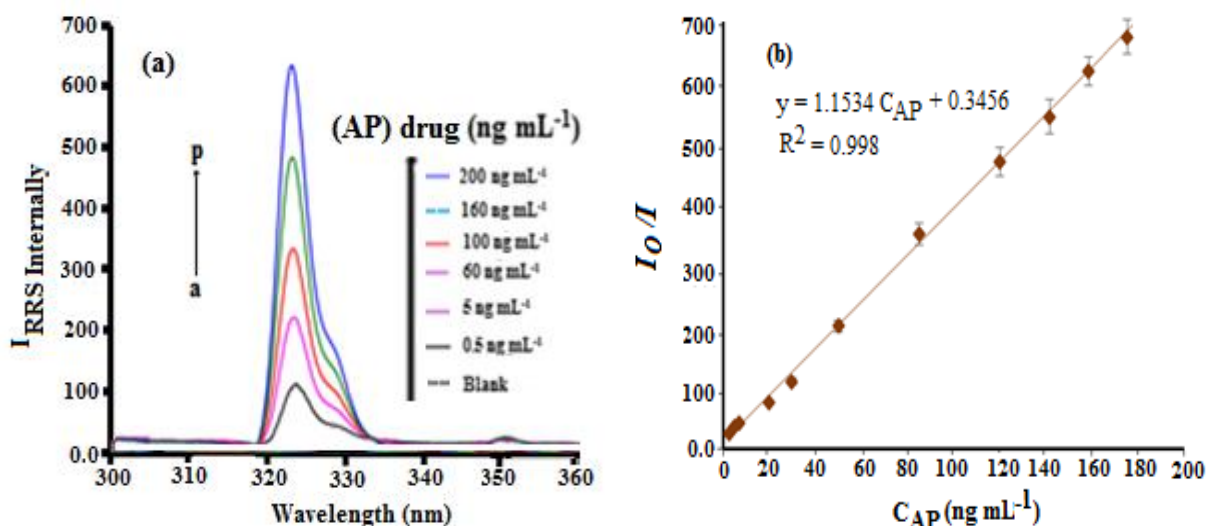


Figure 10. (a) scattering intensity (ΔI_{RRS}) spectra for determination of (AP) drug by chitosan-capped AuNPs in width gap is 10 nm from 0.5 to 200 ng mL⁻¹ (AP) drug (b) Calibration graph from 0.5 to 200 ng mL⁻¹ of (AP) drug. [50.0 ng mL⁻¹ of chitosan-capped AuNPs, pH 6.0, time 5.0 min and phosphate buffer solution].

Optimum values of parameters

The optimum values of parameters is demonstrated in (Table 1). The method can be used as an alternative method for (AP) drug measurement owing to advantages like excellent selectivity, sensitivity, low cost, simplicity, low detection limit, and no need in utilizing organic harmful solvent.

Table 1. Investigation of method repeatability at conditions.

Parameter	Optimum Value for (AP) drug
acetaminophen (AP) drug (M)	(100.0 ng mL ⁻¹)
Chitosan-capped AuNPs (M)	(50.0 ng mL ⁻¹)
pH	6.0
Equilibration time (min)	(5.0 min)
Linear range (LDR)	(0.5 – 200.0 ng mL ⁻¹)
Detection limit (LOD)	(0.5 ng mL ⁻¹)
Relative Standard Deviations (RSD)	(1.1 %)
Advantages	High repeatability, sensitivity, selectivity, wide linear range

Interference studies

Among what we studied were also the interaction between anions, and cations on (AP) drug direction. To perform these studies, various ions were introduced into the solution that contained 100 ng mL of (AP) drug and then applying the general procedure [22].

As exhibited in (Table 2), the tolerance limit was determined as the max concentration of the interfering substance which resulted in an error less than ($\pm 5\%$) for determination of (AP) drug. So selectivity of the recommended method was proven.

Table 2. Limit of tolerance foreign ions on determination of (AP) drug (n=6).

Foreign species	Tolerance limit (ng mL ⁻¹)
Sulfacetamide, Epinephrine, Cyclosporine	500
Amoxicillin, Ampicillin	350
Tramadol, Methadone	150
Pb ²⁺ , Cd ²⁺ , Hg ²⁺	500

Real sample analysis

In order to evaluate the efficiency of the proposed resonance Rayleigh scattering technique which confirmed the accuracy and reliability of the method procedure for trace analysis of (AP) drug existing in real samples according to the instructions mentioned for (AP) drug experiment three, replicates measuring section [35]. The obtained percentage percentiles in (Table 3), indicate that the prepared presented work has a very good performance for determining the (AP) drug in in urine, and blood samples. These results characterized that the new method for determining (AP) drug is appropriate for the quality control, and determination of (AP) drug in urine, and blood samples [31].

Table 3. Detection of (AP) drug in in urine and blood samples with the proposed method (n = 3).

Samples	Added (ng mL ⁻¹)	Founded by RRS (ng mL ⁻¹)	HPLC method (ng mL ⁻¹)	Recovery %
Urine	0.0	2.8 ± 2.4	2.7 ± 2.3	----
	50.0	7.7 ± 1.6		97.6
	100.0	12.7 ± 1.5		99.0
Blood	0.0	3.6 ± 1.5	3.8 ± 1.6	----
	50.0	8.7 ± 1.0		102.0
	100.0	13.6 ± 1.2		102.0
Hospital River water	0.0	2.9 ± 2.2	3.0 ± 2.3	----
	50.0	8.0 ± 1.8		98.0
	100.0	12.9 ± 1.6		97.7

Mean value ± standard deviation, (n = 3).

The recovery was calculated on the basis of the obtained results from resonance Rayleigh scattering (RRS) method.

Conclusions

A describing of method resonance Rayleigh scattering (RRS) for measure of (AP) drug in real samples. This in method of the solution after adding each analyte, distinct stripping peaks can be seen for (AP) drug in the peak separation of at wavelength range of 300–350 nm. This peak was attributed to facilitating electron transfer between (AP) drug, and chitosan-capped AuNPs, and

determination (AP) drug we used from synthesized chitosan-capped AuNPs and Resonance Rayleigh Scattering (RRS) method. A comparison between the proposed method, and the previously published methods for determination (AP) drug by chitosan-capped AuNPs has also, been made for the first time. This method could be suitably used for analysis of (AP) drug in pharmaceutical, human fluid, and hospital samples.

Acknowledgement

We gratefully thank Islamic Azad University Mahshahr Branch, Mahshahr, Iran for financial support.

References

1. Bojko B, Sułkowska A, Maciążek-Jurczyk M, Równicka J, Sułkowski WW. Investigations of acetaminophen binding to bovine serum albumin in the presence of fatty acid: Fluorescence and ¹H NMR studies. *J Mol Struct.* 2009;924-926:332-7.
2. Arabi A, Mohadesi A, Karimi MA, Ranjbar M. Synthesis and Evaluation of Nano Zeolite Na/Al as a New Modifier for Electrochemical Determination of Acetaminophen. *Iran J Anal Chem.* 2022;9(1):88-96.
3. Montaseri H, Forbes PB. Analytical techniques for the determination of acetaminophen: A review. *TrAC, Trends Anal Chem.* 2018;108:122-34.
4. Lim E-B, Vy TA, Lee S-W. Comparative release kinetics of small drugs (ibuprofen and acetaminophen) from multifunctional mesoporous silica nanoparticles. *J Mater Chem B.* 2020;8(10):2096-106.
5. Zhao G, Yang L, Wu S, Zhao H, Tang E, Li C-P. The synthesis of amphiphilic pillar[5]arene functionalized reduced graphene oxide and its application as novel fluorescence sensing platform for the determination of acetaminophen. *Biosensors and Bioelectronics.* 2017;91:863-9.
6. Bu X, Fu Y, Jiang X, Jin H, Gui R. Self-assembly of DNA-templated copper nanoclusters and carbon dots for ratiometric fluorometric and visual determination of arginine and acetaminophen with a logic-gate operation. *Microchim Acta.* 2020;187:1-10.
7. Dikkumbura AS, Aucoin AV, Ali RO, Dalier A, Gilbert DW, Schneider GJ, Haber LH. Influence of acetaminophen on molecular adsorption and transport properties at colloidal liposome surfaces studied by second harmonic generation spectroscopy. *Langmuir.* 2022;38(12):3852-9.

8. Liang SS, Shen PT, Shiue YL, Chang Y-T, Sung P. Development of a Quantitative Method for Monitoring 2-Mercaptobenzothiazole Based on Isotopic Iodoacetamide and Tandem MS. *Curr Anal Chem.* 2020;16(7):947-54.
9. Murillo Pulgarín JA, Alañón Molina A, Jiménez García E, García Gómez L. A sensitive resonance Rayleigh scattering sensor for dopamine in urine using upconversion nanoparticles. *J Raman Spectrosc.* 2020;51(3):406-13.
10. Parham H, Khoshnam F. Solid phase extraction–preconcentration and high performance liquid chromatographic determination of 2-mercapto-(benzothiazole, benzoxazole and benzimidazole) using copper oxide nanoparticles. *Talanta.* 2013;114:90-4.
11. Xiong M, Rong Q, Meng H-m, Zhang X-b. Two-dimensional graphitic carbon nitride nanosheets for biosensing applications. *Biosensors and Bioelectronics.* 2017;89:212-23.
12. Zhang K, Lv S, Zhou Q, Tang D. CoOOH nanosheets-coated g-C₃N₄/CuInS₂ nanohybrids for photoelectrochemical biosensor of carcinoembryonic antigen coupling hybridization chain reaction with etching reaction. *Sens Actuators, B.* 2020;307:127631.
13. Shahrouei F, Elhami S, Tahanpesar E. Highly sensitive detection of Ceftriaxone in water, food, pharmaceutical and biological samples based on gold nanoparticles in aqueous and micellar media. *Spectrochim Acta, A.* 2018;203:287-93.
14. Abdel-Lateef MA, Derayea SM, El-Deen DAN, Almahri A, Oraby M. Investigating the interaction of terbinafine with xanthenes dye for its feasible determination applying the resonance Rayleigh scattering technique. *Roy Soc Open Sci.* 2021;8(1):201545.
15. Mohammed BS, Derayea SM, Hassan YF, A. Abu-hassan A. Resonance Rayleigh scattering approach based on association complex formation with erythrosine B for determination of venlafaxine, application to the dosage form and spiked human plasma. *Luminescence.* 2022;37(7):1215-22.
16. Parham H, Saeed S. Resonance Rayleigh scattering method for determination of ethion using silver nanoparticles as probe. *Talanta.* 2015;131:570-6.
17. Parham H, Pourreza N, Marahel F. Resonance Rayleigh scattering method for determination of 2-mercaptobenzothiazole using gold nanoparticles probe. *Spectrochim Acta, A.* 2015;151:308-14.
18. Sun R, Wang Y, Ni Y, Kokot S. Graphene quantum dots and the resonance light scattering technique for trace analysis of phenol in different water samples. *Talanta.* 2014;125:341-6.
19. Yang J, Wang E, Zhou S, Yang Q. Effects of (R)-and (S)-propranolol hydrochloride enantiomers on the resonance Rayleigh scattering spectra with erythrosine B as probe and their analytical applications. *Talanta.* 2015;134:754-60.

20. Salem H, Elsoud FAA, Heshmat D, Magdy A. Resonance Rayleigh scattering technique-using erythrosine B, as novel spectrofluorimetric method for determination of anticancer agent nilotinib: application for capsules and human plasma. *Spectrochim Acta, A.* 2021;251:119428.
21. Kazemi Z, Marahel F, Hamoule T, Mombeni Goodajdar B. Design and Evaluation an *Origanum majorana*-Capped AgNPs Sensor: Determination of Trace Megestrol Drug in Urine and Blood Samples using Kinetic Spectrophotometric Method. *J Appl Chem Res.* 2022;16(1):30-47.
22. Pargari M, Marahel F, Goodajdar BM. Applying Kinetic Spectrophotometric Method and Neural Network Model for the Quantity of Epinephrine Drug by Starch-capped AgNPs Sensor in Blood and Urine Samples. *Russ J Anal Chem.* 2022;77(4):482-92.
23. Hatamie A, Marahel F, Sharifat A. Green synthesis of graphitic carbon nitride nanosheet (g-C₃N₄) and using it as a label-free fluorosensor for detection of metronidazole via quenching of the fluorescence. *Talanta.* 2018;176:518-25.
24. Ramzannezhad A, Hayati A, Bahari A, Najafi-Ashtiani H. Magnetic detection of albuminuria using hematite nanorods synthesized via chemical hydrothermal method. *Iran J Basic Med Sci.* 2021;24(7):962.
25. Marahel F. Designed a Spectrophotometric Method for the Determination of Tartrazine Residual in Different Drinks and Foodstuffs by Using Mandarin leaves-capped Gold Nanoparticles. *Iran J Chem Chem Eng.* 2022;41(12):4108-21.
26. Farkhari N, Abbasian S, Moshaii A, Nikkhah M. Mechanism of adsorption of single and double stranded DNA on gold and silver nanoparticles: investigating some important parameters in bio-sensing applications. *Colloid Surfaces B.* 2016;148:657-64.
27. Patra JK, Baek K-H. Novel green synthesis of gold nanoparticles using *Citrullus lanatus* rind and investigation of proteasome inhibitory activity, antibacterial, and antioxidant potential. *Int J Nanomed.* 2015:7253-64.
28. Li Q, Tan X, Fu L, Liu Q, Tang W. A novel fluorescence and resonance Rayleigh scattering probe based on quantum dots for the detection of albendazole. *Anal Methods.* 2015;7(2):614-20.
29. Masoudyfar Z, Elhami S. Surface plasmon resonance of gold nanoparticles as a colorimetric sensor for indirect detection of Cefixime. *Spectrochim Acta, A.* 2019;211:234-8.
30. Bouroumand S, Marahel F, Khazali F. Designed a Fluorescent Method by Using PbS with Gelatin via Quantum Dots for the Determination of Phenylpropanolamine Drug in Human Fluid Samples. *J Appl Chem Res.* 2022;16(3):57-71.
31. Karpova S, Blazheyevskiy MY, Mozgova O, Ivashura M. The kinetic spectrophotometric method for the determination of azlocillin in solutions. *Вісник фармації.* 2019(1):15-9.

32. Zhu Y-P, Ren T-Z, Yuan Z-Y. Mesoporous phosphorus-doped g-C₃N₄ nanostructured flowers with superior photocatalytic hydrogen evolution performance. *ACS Appl Mater Inter.* 2015;7(30):16850-6.
33. Zhu Z, Yu Y, Dong H, Liu Z, Li C, Huo P, Yan Y. Intercalation effect of attapulgite in g-C₃N₄ modified with Fe₃O₄ quantum dots to enhance photocatalytic activity for removing 2-mercaptobenzothiazole under visible light. *ACS Sustain Chem Eng.* 2017;5(11):10614-23.
34. Hamad AE, Mohammed BS, Derayea SM, El-Malla SF. Micelle sensitized synchronous spectrofluorimetric approaches for the simultaneous determination of simeprevir and ledipasvir: Application to pharmaceutical formulations and human plasma. *Spectrochim Acta, A.* 2020;239:118471.
35. Muldrew KL, James LP, Coop L, McCullough SS, Hendrickson HP, Hinson JA, Mayeux PR. Determination of acetaminophen-protein adducts in mouse liver and serum and human serum after hepatotoxic doses of acetaminophen using high-performance liquid chromatography with electrochemical detection. *Drug Metab Dispos.* 2002;30(4):446-51.